Hindawi
International Journal of Polymer Science
Volume 2022, Article ID 9634929, 15 pages
https://doi.org/10.1155/2022/9634929

Research Article

Impact of Fiber Buildup Stacking Sequence on Thermo-Mechanical Behaviour of Natural Fiber–Reinforced Anamide Composites

M. Subramanian,[1] **M. Diviya**,[2] **S. Kaliappan**,[3] **A. Deepak**,[4] **Kuldeep K. Saxena**,[5] **and Nasim Hasan**[6]

[1]*Department of Mechanical Engineering, St. Joseph's College of Engineering, Chennai, Tamil Nadu, India*
[2]*Department of Computer Science and Engineering, Amrita School of Computing, Amrita Vishwa Vidyapeetham, Chennai, Tamil Nadu, India*
[3]*Department of Mechanical Engineering, Velammal Institute of Technology, Chennai, Tamil Nadu, India*
[4]*Department of Electronics and Communication Engineering, Saveetha School of Engineering, Saveetha School of Medical and Technical Sciences, Chennai, Tamil Nadu, India*
[5]*Department of Mechanical Engineering, GLA University, Mathura, Uttar Pradesh, India*
[6]*Mettu University, Mettu, Oromia P. O. Box 318, Ethiopia*

Correspondence should be addressed to M. Subramanian; subramanianm@stjosephs.ac.in
and Nasim Hasan; nasim.hasan@meu.edu.et

Received 26 March 2022; Revised 7 July 2022; Accepted 15 October 2022; Published 7 November 2022

Academic Editor: Andrea Camposeo

This article focuses on the viscoelastic behaviour of the anamide composites using a dynamic mechanical study developed by hot compression moulding technology at higher temperatures. The frequency range for this analysis is 1 Hz. In the nitrogen atmosphere, thermogravimetry analysis differential scanning calorimetry was used to investigate the thermal stability of composite laminates with various fiber orientations. The findings showed that a glass transition temperature close to 100°C can be achieved at 1 Hz to increase the fiber orientation of the basalt fiber-enhanced anamide compounds. Through the thermogravimetric analysis experiments, the excellent thermal stability of composite laminates at temperatures above 600°C was conspicuous. Analysis using the Fourier transform infrared (FTIR) spectroscopy envisioned the surface chemical properties of anamide films at various fiber orientations, and the interaction properties between fiber and matrix were determined. Scanning electron microscopy on composite laminate surfaces proclaimed that the interface relationship between the basalt fiber and the anamide material is superior with FTIR findings being assisted. The findings demonstrate that composite laminates may be a good replacement for high-performance and high-temperature applications since they are thermally extremely robust with great rigidity.

1. Introduction

Nearly every sector, such as aerospace, aircraft, maritime, and transportation, has tremendous demand for creativity in the production of high-performance content coupled with lightweight, high-power, mechanical, electrical, thermal, and environmental aspects [1]. Advanced composites offer a hallmark for creative science solution. Basalt fiber–reinforced thermoplastic (BFRT) composites have been getting a lot of attention over the past ten years. This is due to the fact that, in comparison to other fiber-reinforced thermoplastics, BFRT composites have more desirable characteristics, including higher levels of strength and stiffness as well as improved impact resistance [2, 3]. The rock known as basalt comes from

volcanic activity. The fiber that is created from basalt rock is highly cost-effective and possesses a lot of good features, including being inflammable, absorbing sound, providing thermal insulation, and being biologically stable [4].

The poor thermal tolerance and usually their low temperature properties, mainly due to the weak thermal resistance of the polymer matrix, are the key inconveniences of the fiber reinforced polymer (FRP) composites. The thermal activity of the FRP composites is thermal monitoring of the material properties according to temperature and surface calculation within such temperature ranges or in a particular isothermal scenario. The common studies in this area include dynamic mechanical analysis (DMA) and thermogravimetric analysis (TGA). Product habits are usually based on elevated temperatures. DMA is used for the rheological study of materials. Product properties, such as storage modulus, loss modulus, tanδ, and transformation temperature (T_g), can be calculated using this methodology under varying temperatures, speeds, pressures, and modes of deformation. Therefore, DMA will investigate the characteristics of viscoelastic components, such as polymers. The word viscoelastic describes materials that exhibit elastic and viscous properties when deformed. In structural applications where cyclic loading is critical, BFRTs are employed increasingly often. This necessitates a rigorous evaluation of the viscoelastic and thermomechanical behaviours of the composite materials.

When determining whether or not a material is suitable for a particular structural application, the viscoelastic behaviour of polymer composites is an essential factor to consider. By altering the load, frequency, and temperature, DMA has been used to investigate the viscoelastic behaviour of composite materials [5]. The basalt fiber had a good impact on the mechanical qualities as well as the damping properties. They also found that the composite configuration in which the basalt was placed on the skin had superior mechanical and damping capabilities compared to the other configurations of the composite [6]. Numerous studies on the dynamic mechanical response of basalt fibers demonstrated that altering the orientation of basalt fibers inside the polymer assists results in a reduction in the modulus and has an effect on the loss factor. Lu et al. [7] performed DMA on BFRP surfaces. DMA was used in the form to examine the viscoelastic nature and structural properties of polymer–metal matrix composites in order to evaluate their respective damping and rigidity characteristics [8–11]. Research demonstrates that the piling pattern and fiber orientation influence the complex mechanical properties of the composite hybrid polymer. Over a variety of temperatures and frequencies [12–16], these complex properties are noteworthy.

Several studies around the world have studied how thermosetting polymers have been influenced by fiber orientation distribution to thermally and mechanically examine reinforced fibers. This study focuses on the different fiber orientations on the complex behaviour of basalt fiber–reinforced anamide composite laminates. The laminates were designed using the technique of compression moulding, and their complex mechanical properties were calculated in terms of volume modulus, failure modulus, and tanδ. In addition, a study on differential scanning calorimetry (DSC) and thermogravimetry (TG) was conducted to evaluate the thermal stability and exploration of the composite laminate decomposition under various orientations. The research on the impact of fiber orientation on FTIR actions is restricted and can evaluate the properties of the surface interaction between the fiber and the matrix.

Table 1: Physical properties of the basalt fiber.

Dry density (g/cm^3)	2.40
Diameter (μm)	10–20
Modulus of elasticity (GPa)	105
Breaking strength (MPa)	3500
Elongation at break (%)	2.5

Table 2: Properties of anamide resin.

Specific gravity at 30°C	1.00–1.20
Viscosity at 30°C, spindle no. 6, 100 rpm (cPs)	2000–5000
Acid value (mgKOH/g)	140–170
(a) Solid content at 210°C/3 hours (%)	55–60
(b) Solid content at 140°C/15 minutes (%)	70–75
T_g of neat resin by MDSC (°C)	344

2. Materials and Methods

2.1. Basalt Fiber. Basalt fiber is a naturally occurring volcanic rock fiber obtained by the accelerated cooling of molten lava and discovered its way as a fiber showing very strong thermal properties, such as high-temperature tolerance and thermal resilience, that finds its use as insulating fibers in refractory linings, aircraft, automobile, marine, and civil structures. This consists of minerals that exist naturally, including plagioclase, olivine, and pyroxene. Basalt fiber output initially involves rock grinding, washing, and heating to 1500°C temperature. This is then extruded, under which the operation becomes easier and more energy-efficient compared with other fiber types. Generally, the extruded fibers are inside the 10–20 μm [17, 18] dimension scale. Anakaputhur Weavers Association procured the basalt fibers used in the manufacture of composites. Table 1 demonstrates the physical properties of the basalt fiber [19].

2.2. Anamide Resin. Anamide is a common portion of a polyimide binder resin comprising dissolved monomeric reactants in polar aprotic solvents. The binder compound is ideal for construction products constructed from fiber-polyimide. The strong chemical stability of the imide chain, the repeated element in polyimide polymeric molecules, gives the polymer a good thermal stability and thermo-oxidant stability. Polyimides often exhibit a strong intermolecular cohesive force owing to the contact between the chains in charge transition. It results in very strong mechanical toughness in the composites. Basalt-polyimides have very poor interference with electromagnetic signals owing to a weak dielectric constant, rendering it invisible to

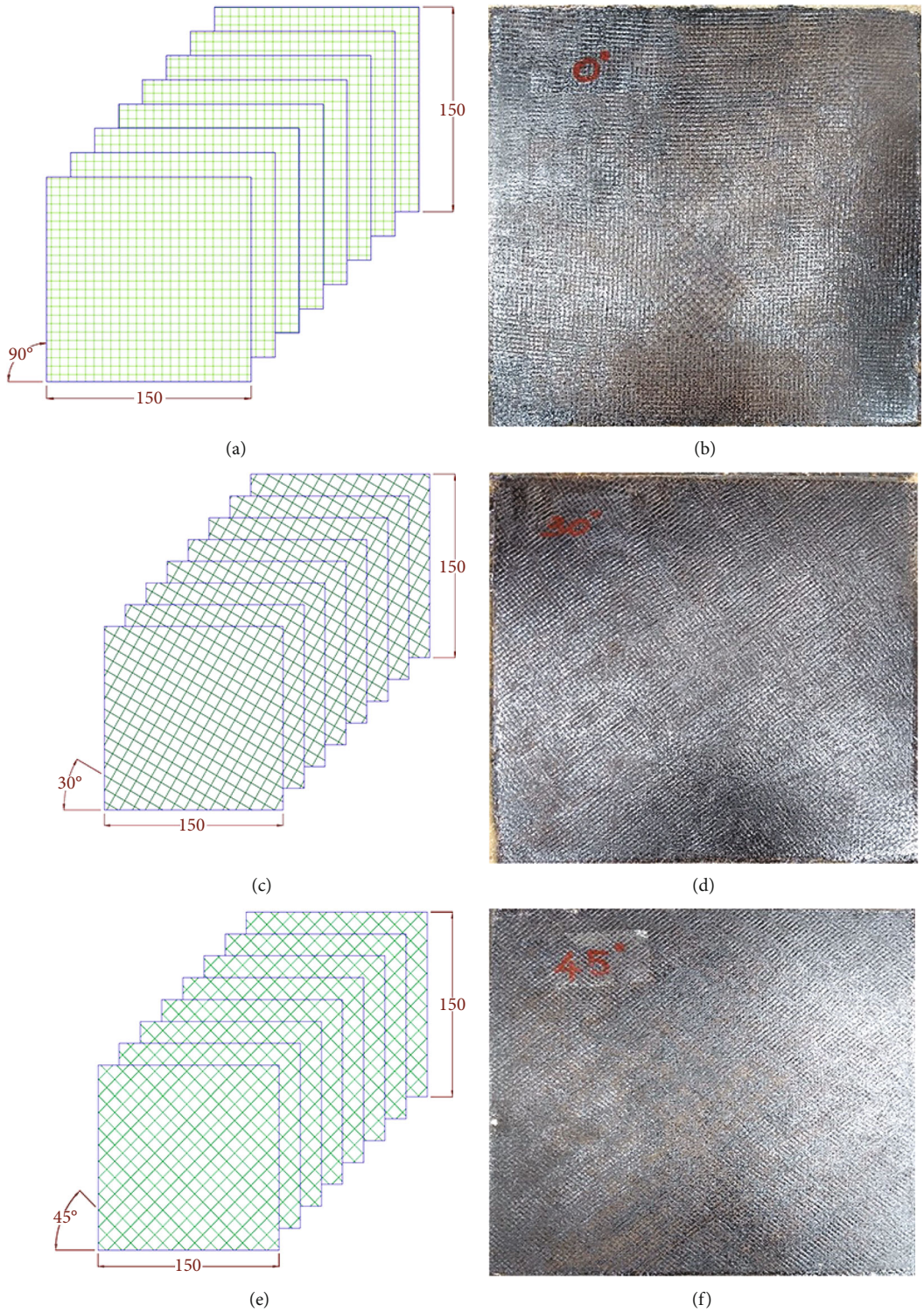

Figure 1: Fabricated basalt fiber–reinforced anamide composites at different fiber orientations (a) and (b) 0°/90° fiber orientation, (c) and (d) 30°/120° fiber orientation, and (e) and (f) 45°/135° fiber orientation.

electromagnetic radiation. Such a mixture of properties renders polyimides a special commodity suitable to critical applications of aerospace. These lightweight materials are used in the manufacture of airframe parts and radomes of high temperature. Over longer durations, these composite materials may tolerate temperatures of up to 320°C. Table 2 displays the properties of anamide procured from Anabond India Private Limited, Chennai, Tamil Nadu, India, and was used for manufacturing purposes.

2.3. Fabrication of Composites. The composite plate of different orientations, including 0°/90°, 30°/120°, and 45°/135°, is

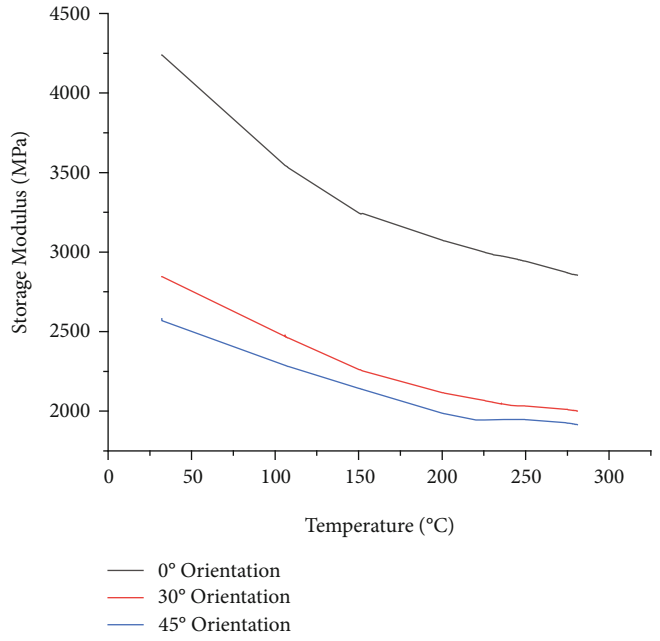

Figure 2: Temperature versus storage modulus of the basalt fiber reinforced with anamide composites at different orientations and a frequency of 1 Hz.

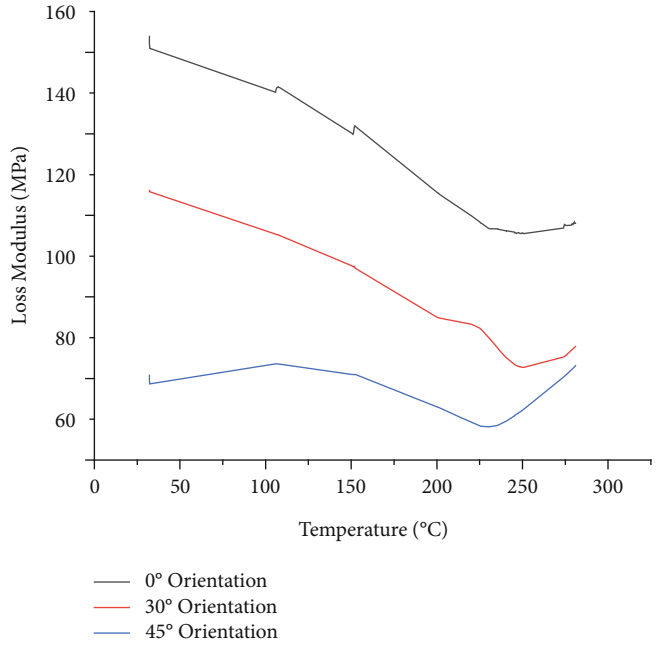

Figure 3: Temperature versus loss modulus of the basalt fiber reinforced with anamide composites at different orientations and a frequency of 1 Hz.

designed using compression moulding techniques. The necessary volume of basalt fiber is determined, and their weight is assessed for different orientations, as shown in Figure 1. The fiber weight is weighed as 60% of the overall weight, and the other 40% as the anamide resin weight. The fraction of the fiber volume is determined using the mixture law to get optimum bonding power. More than 40% change in weight percentage of anamide resin results in the creation of voids that impact the bonding. Since the anamide resin has a higher viscosity density of around 2000–5000 cPs at 30°C and 100 rpm, the application over the fiber is rough. For dilution, ethanol (C_2H_5OH) is applied in the ratio of 1 : 1 to prevent the challenge. The combination (resin and ethanol) is well mixed such that the resin is not sedimented. The fiber is put over the release substrate, which is covered with release agent (Teflon-coated silicon fiber glass) to avoid premature adhesion of the sticky sheet. The resin is sprayed evenly on both sides of the fiber and alloyed at 30°C for 24

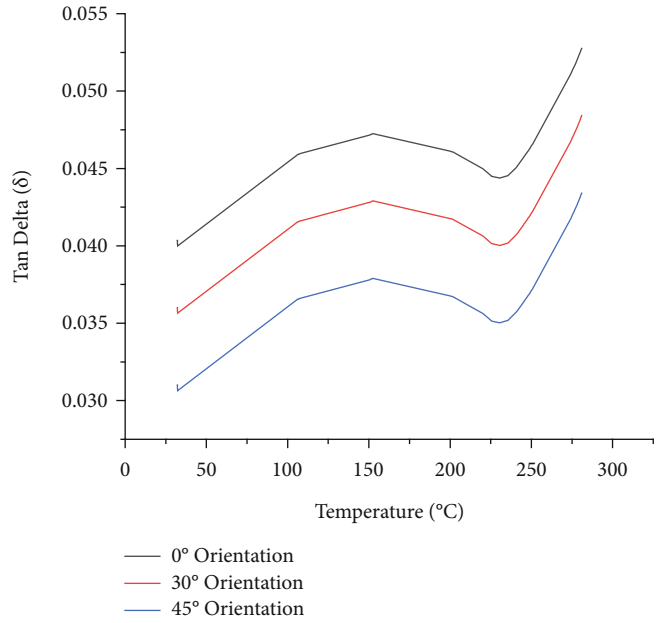

Figure 4: Temperature versus tanδ of the basalt fiber reinforced with anamide composites at different orientations and a frequency of 1 Hz.

hours to cure. Shrinkage is contained on the fabric, owing to the resin's stronger adhesive quality. The rolling method is done with a 4 mm diameter and 15 mm roller, by manually adding constant pressure to prevent shrinking. Following the levelling process, release paper is put over the fiber to mark the fiber orientation and measurements, and the fiber is extracted from the sheet with the correct orientation and length. The moulding die is made from cast iron with an outward length of 150 mm × 150 mm and an outward space of 5 mm. The dies are capable of withstanding both heavy pressure and low temperatures. To resist adhesion, the die is covered with Teflon powder. Each layer is inserted into the die and compressed over another. Upon each layer addition, the levelling is performed manually in the roller. When the correct volume of layer has been introduced into the die degassing process, the excess solvent and air bubbles are separated from the layers. It is finished 20 minutes in the vacuum oven that is run at 120°C. Degassing eliminates the unnecessary solvents from the composites, during which the die is placed on mould with microcontroller PR502 under hydraulic strain. The whole programming is fed in 15 stages inside the microcontroller. The scale of the mould is 160 mm × 160 mm , the piston diameter is 57.6 cm, and the mould surface is 263.59 cm^2. To limit heat loss throughout the cycle, the moulding die is lined with glass cloth. The cycle started at 30°C ambient temperature and increased to 80°C within 10 minutes, then kept for 30 minutes to achieve uniform distribution of temperature around the specimen. Within another 10 minutes, the mercury increased to 100°C again and stayed at the same level for 120 minutes. In addition, in another 25 minutes, temperature increased to 150°C and stayed for 60 minutes. The holding is performed at 170°C for 60 minutes, and the oil pressure of 100 kg/cm^2 is slowly added at the top. Covalent bond and ionic bond break down at a temperature of 170°C. Temperature falls again to 200°C and stays in place for 20 minutes. The oil pressure is then raised again at 240°C. This time the pressure is raised to 150 kg/cm^2 and kept for 60 minutes, and the anamide resin starts to cure at this point. It tends to improve the binding tension between resin and fiber when adding oil pressure friction between the layers. The same temperature is held for 180 minutes, until the temperature exceeds 330°C. Curing cycle was done at 330°C, and the quality of the composite material is greater as a result. Cooling is permitted on the specimen. The heaters are turned off, and oil pressure is released at 100°C.

2.4. Dynamic Mechanical Analysis. A DMA Q800 V20.4 BUILD 24 dynamic mechanical analyzer was utilized to examine the viscoelastic properties of basalt fiber–reinforced anamide composite laminates at various fiber orientations. Complex mechanical research was done in compliance with the standard ASTMD 4065. The research sample measurements used were 35 × 14 × 3.5 mm^3. The laminates experienced three-point bending at 1 Hz frequency under a regulated sinusoidal charge setting. Set pressure, single frequency study ended a temperature spectrum ranging between 30 and 300°C at a constant heating rate of 10°C/minute.

2.5. TG–DTG–DSC Analysis. A thermo-gravimetric analyser (NETZSCH STA 449F3) as per ASTM specification E1131-03 was used to examine the thermal quality of the basalt fiber–reinforced anamide composite under specific fiber orientation. The composites (8.5 mg) were put in an alumina crucible as per the procedure and followed a pyrolysis cycle in a safe atmosphere with nitrogen. The dose of N_2 flow used for this method is 20 mL/minute. The study was carried out at a steady heating rate of 10°C/minutes, from room temperature to 1000°C. DSC work was conducted using a DSC

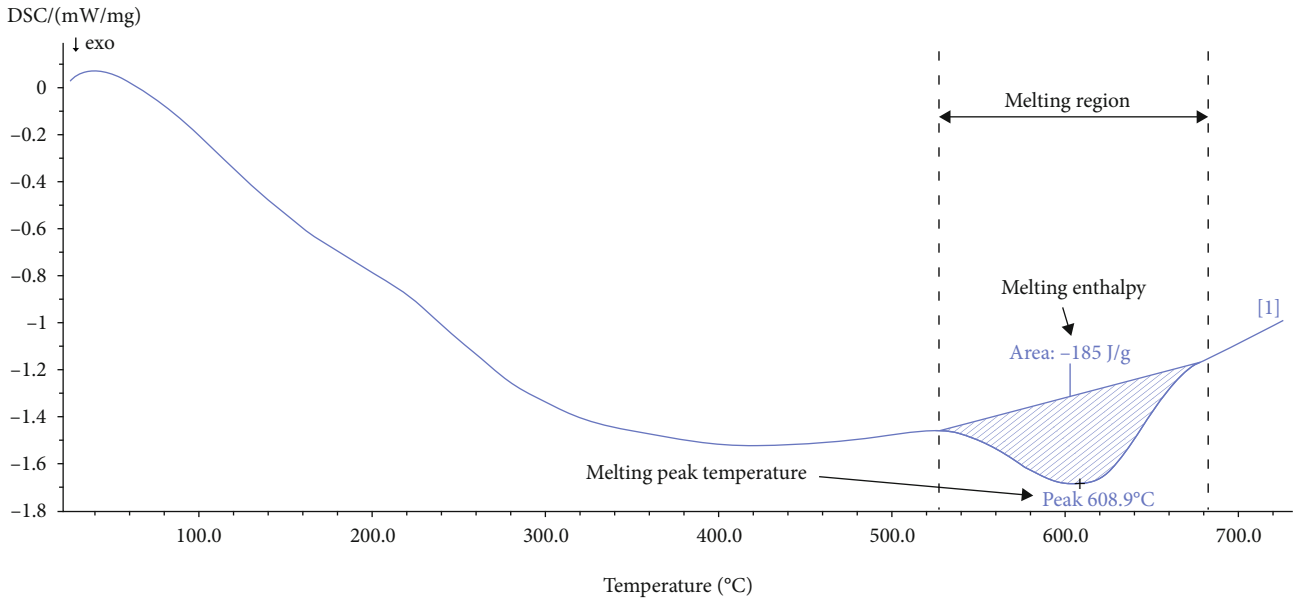

(a)

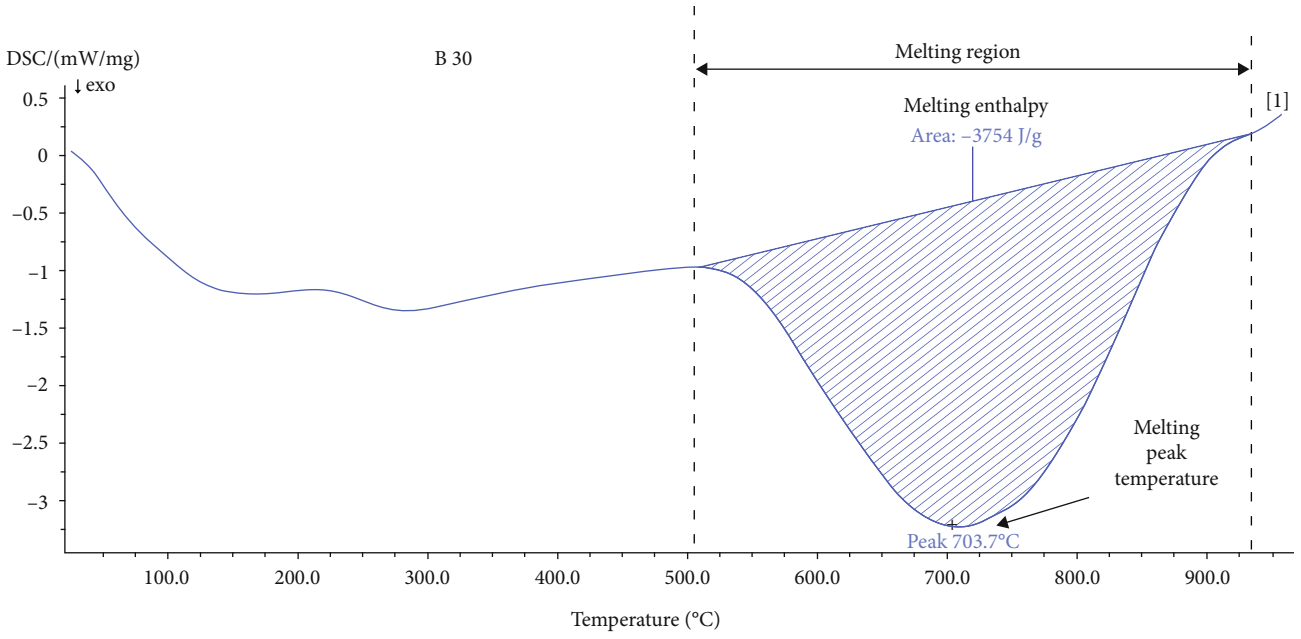

(b)

Figure 5: Continued.

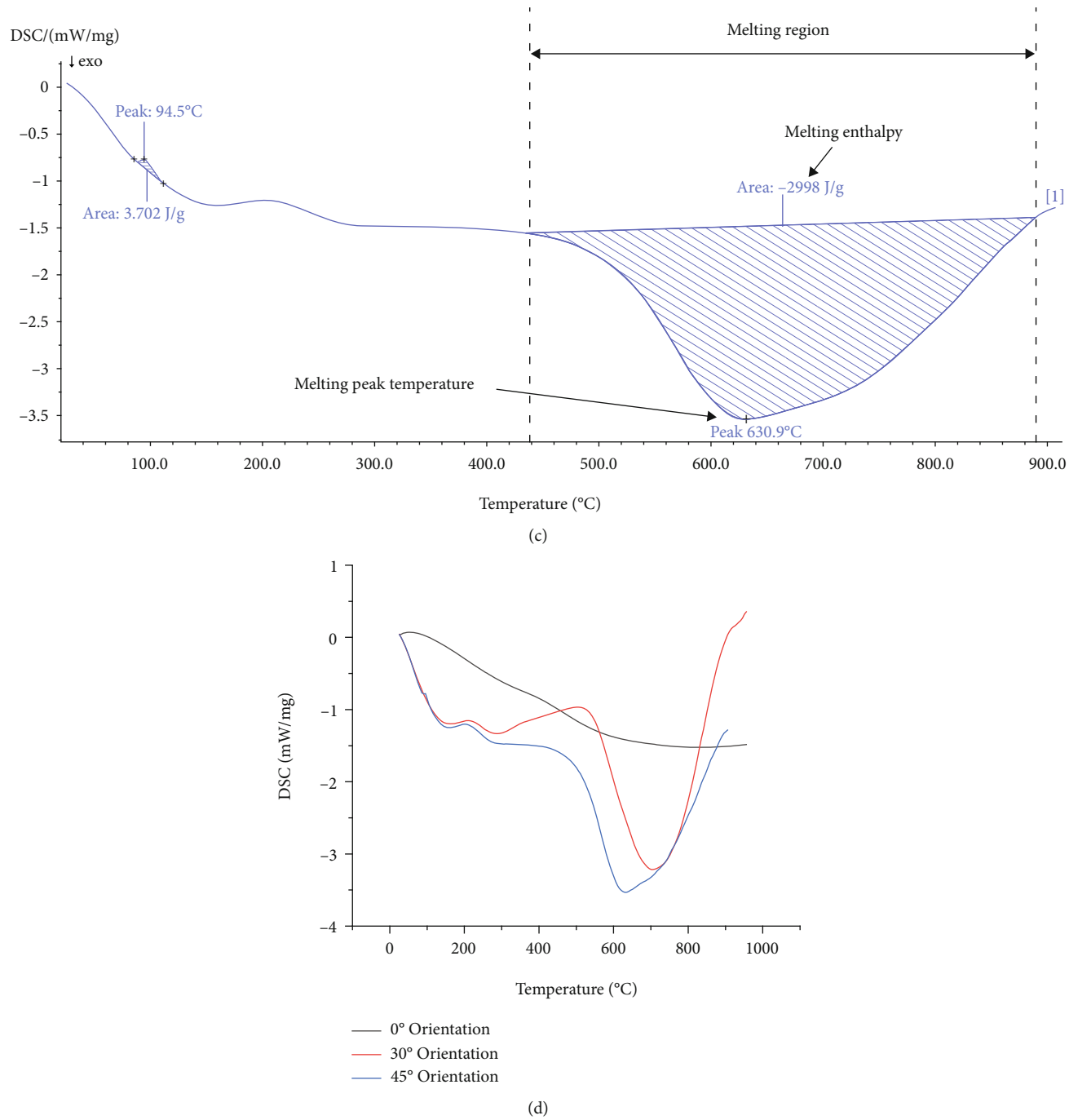

Figure 5: DSC plot for basalt fiber–reinforced anamide composites (a) 0° orientation, (b) 30° orientation, (c) 45° orientation, and (d) comparison graph.

analyser NETZSCH STA 449F3. Within the crucible pan made from Al_2O_3 (alumina) was mounted a composite sample of 8.5 mass/mg. Another crucible pan was used without sample as a guide. Under the nitrogen safe condition (flow rate 20 mL/minute), the DSC check was conducted at a heating rate of 10°C/minutes from room temperature to 1000°C.

2.6. FTIR Analysis of Composites. Throughout the entire test, a Fourier transform infrared (FTIR) spectrophotometer (Bruker IFS125HR) was used. The fiber-reinforced polymer was ground into powder with KBr infrarot grade powder (50 mg) and placed into a measuring pellet. As a consequence, long-term scanning was used to solve composite peaks, and the signal-to-noise ratio of the coded spectrum was adequate. With a resolution of 1 cm^{-1}, growing spectrum was measured within the range of 450–4000 cm^{-1}. Subtracted from the sample spectrum was the source distribution of KBr pellet.

Table 3: Thermal endurance at different orientations of basalt fiber–reinforced anamide composites.

Orientation (°)	Melting enthalpy (J/g)	Melting peak temperature (°C)	Residual mass (%)
0	−185	608.9	92.98 at 726.2°C
30	−3754	703.7	86.70 at 959.1°C
45	−2998	630.9	83.90 at 908.6°C

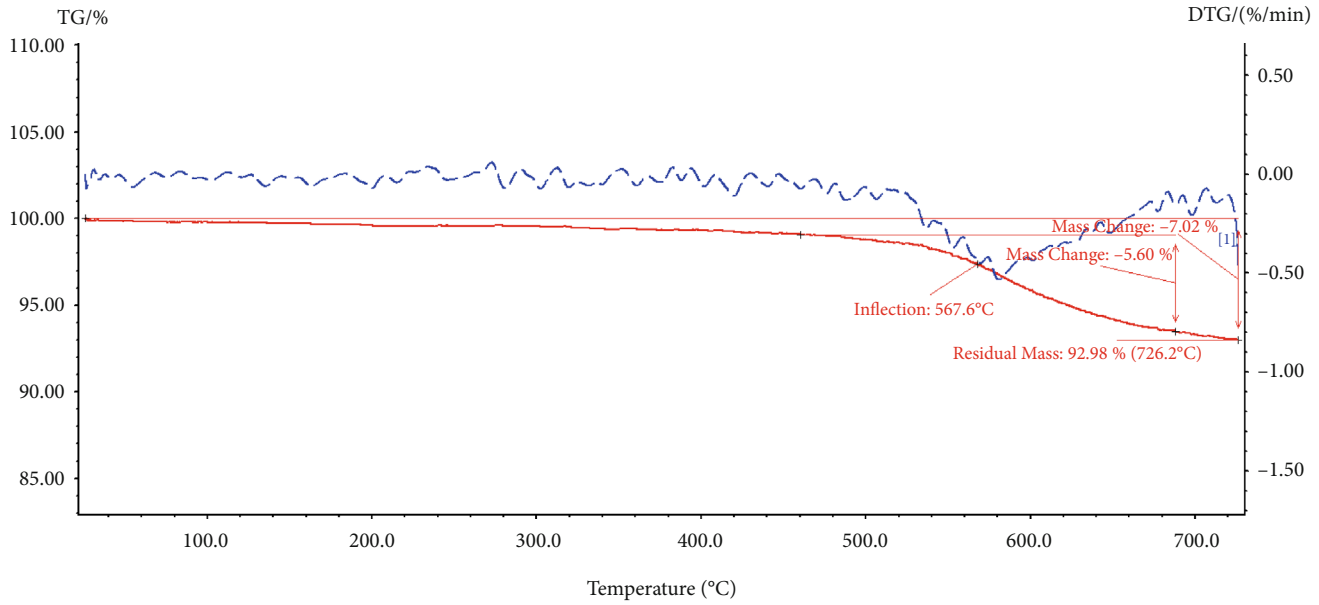

(a)

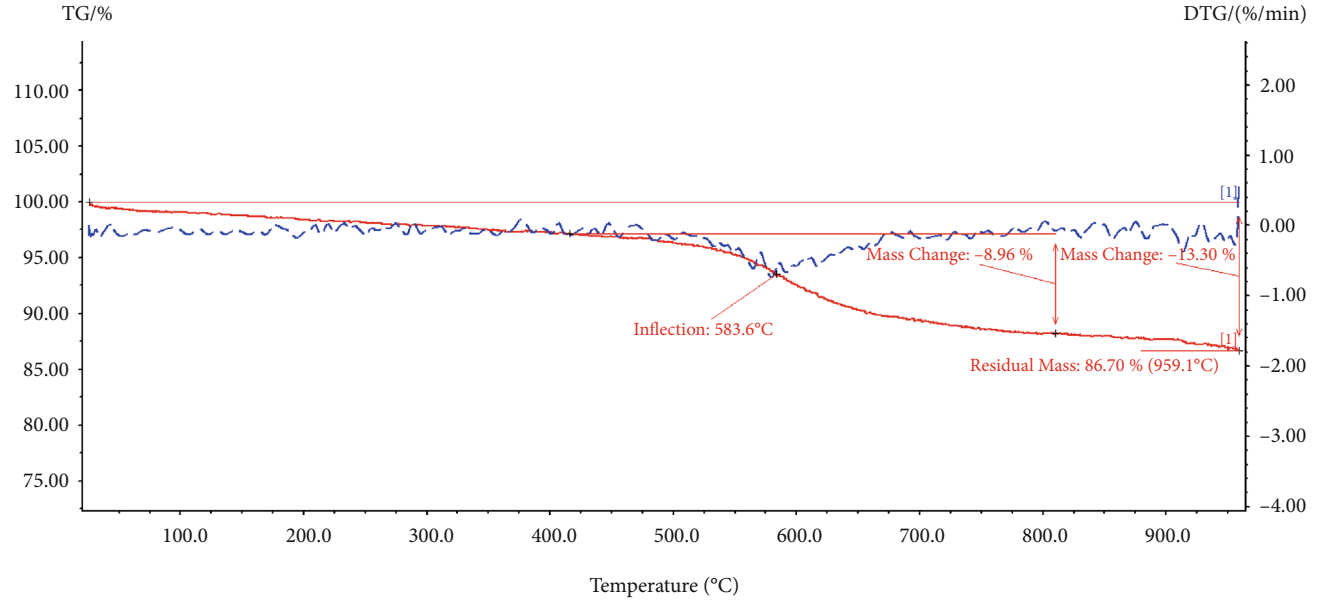

(b)

Figure 6: Continued.

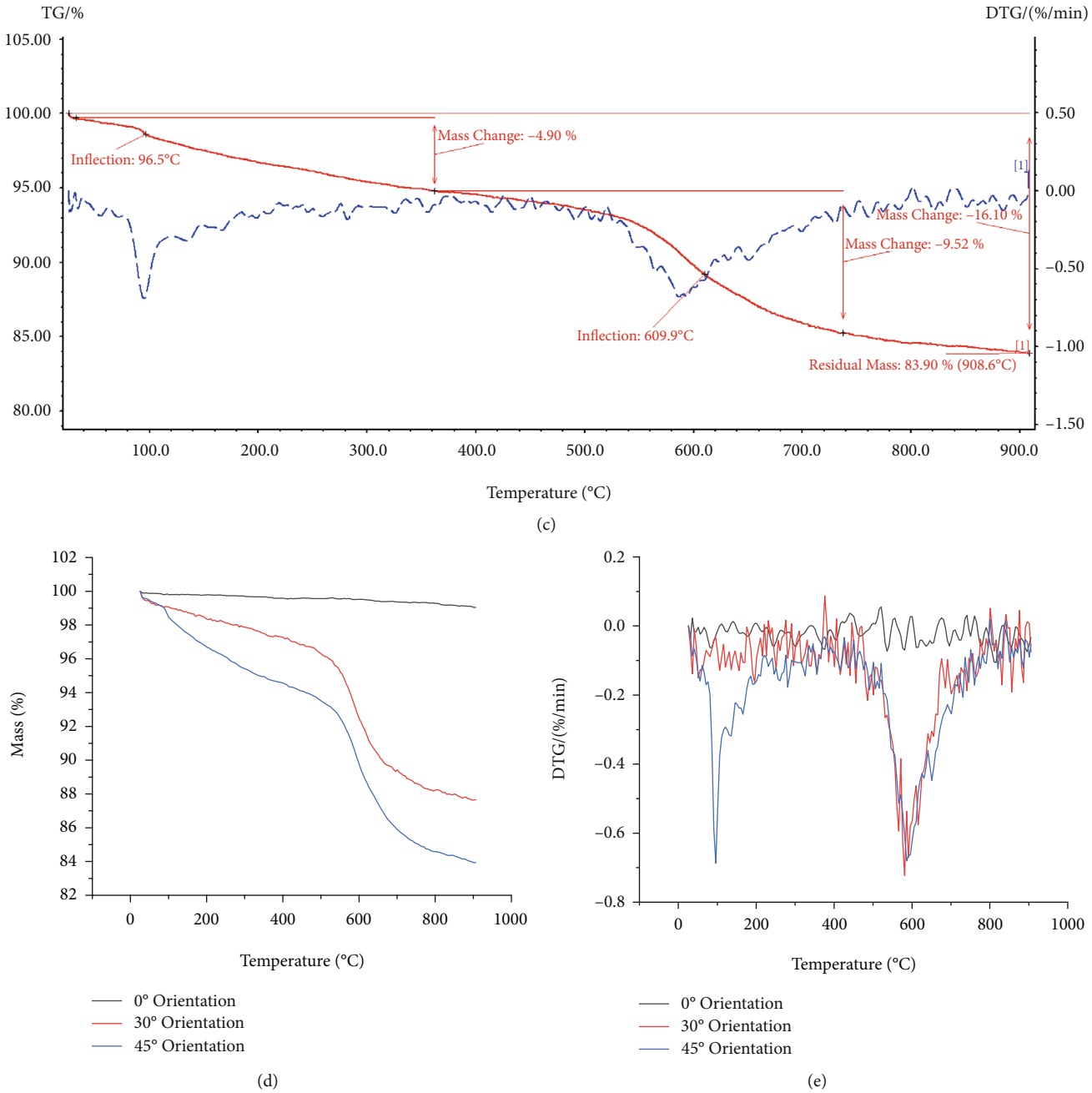

Figure 6: Thermal stability of basalt fiber–reinforced anamide composites at (a) 0° orientation, (b) 30° orientation, (c) 45° orientation, (d) temperature versus residual mass for different orientations, and (e) temperature versus DTG for different orientations.

3. Results and Discussion

3.1. Effect of Fiber Orientation on DMA. Some of the most important factors in evaluating the dynamic mechanical properties of fiber-reinforced polymer composites are the alignment of the fibers with respect to the loading path. Figures 2, 3 and 4 provide a study on the elastic properties of composite structure for varying fiber orientations (0, 30, and 45°) at a frequency of 1 Hz. It is assumed that the storage module has a drastic decrease in its values varying from 4000 to 2600 MPa with an improvement in fiber orientation attributable to the fiber bending resistance in the matched orientations. The dynamic storage modulus (E') is known as stress in distribution with strain divided by strain in sinusoidal shear distortion. Figure 2 indicates the differences in the storage modulus as the temperature feature for the analyzed composites at a frequency of 1 Hz. When temperature increases, storage modulus (E') diminishes for all composites of different orientations, and this is due to improved molecular stability of polymer chains and reduced resin stiffness [20]. A significant drop is anticipated for unfilled device because the toughness at elevated temperature is calculated by the amorphous area, which is quite less regarding

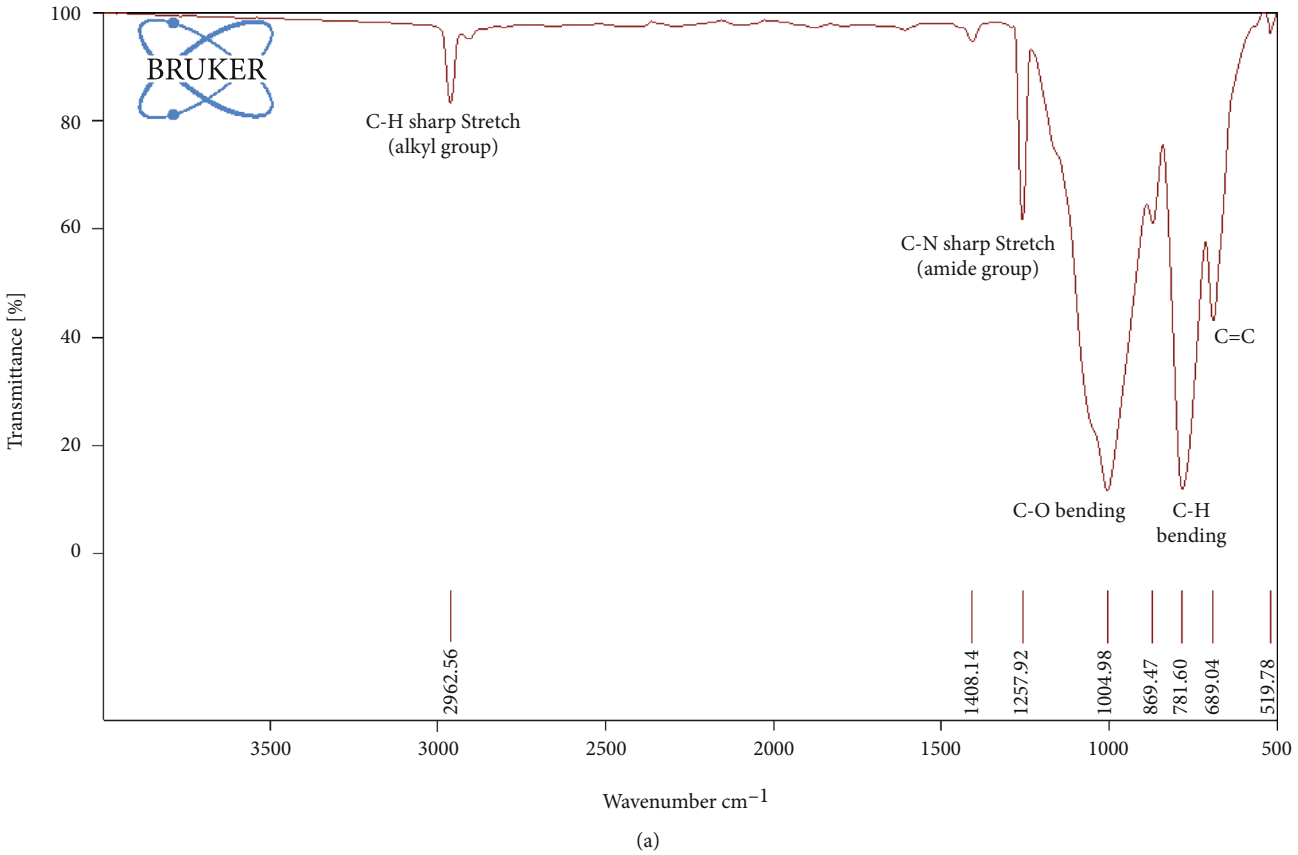

(a)

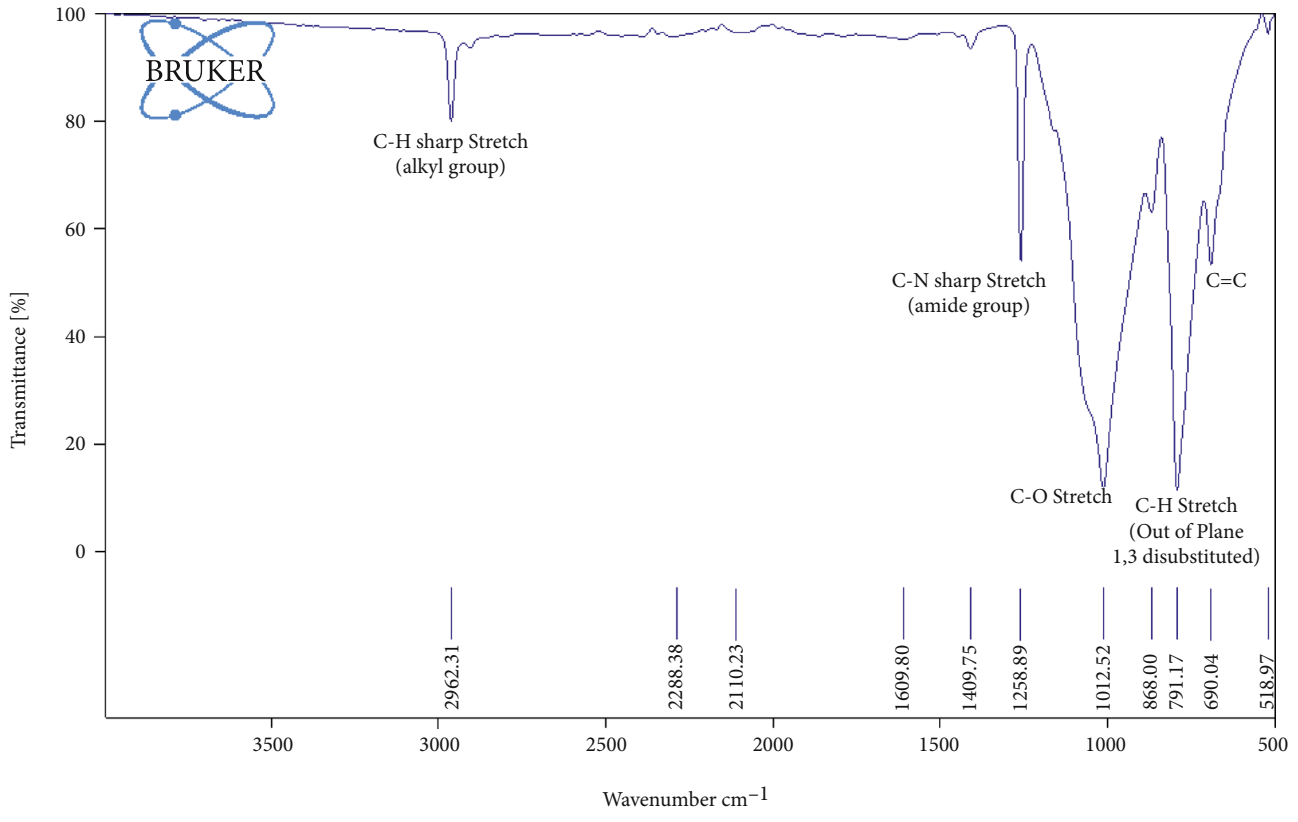

(b)

Figure 7: Continued.

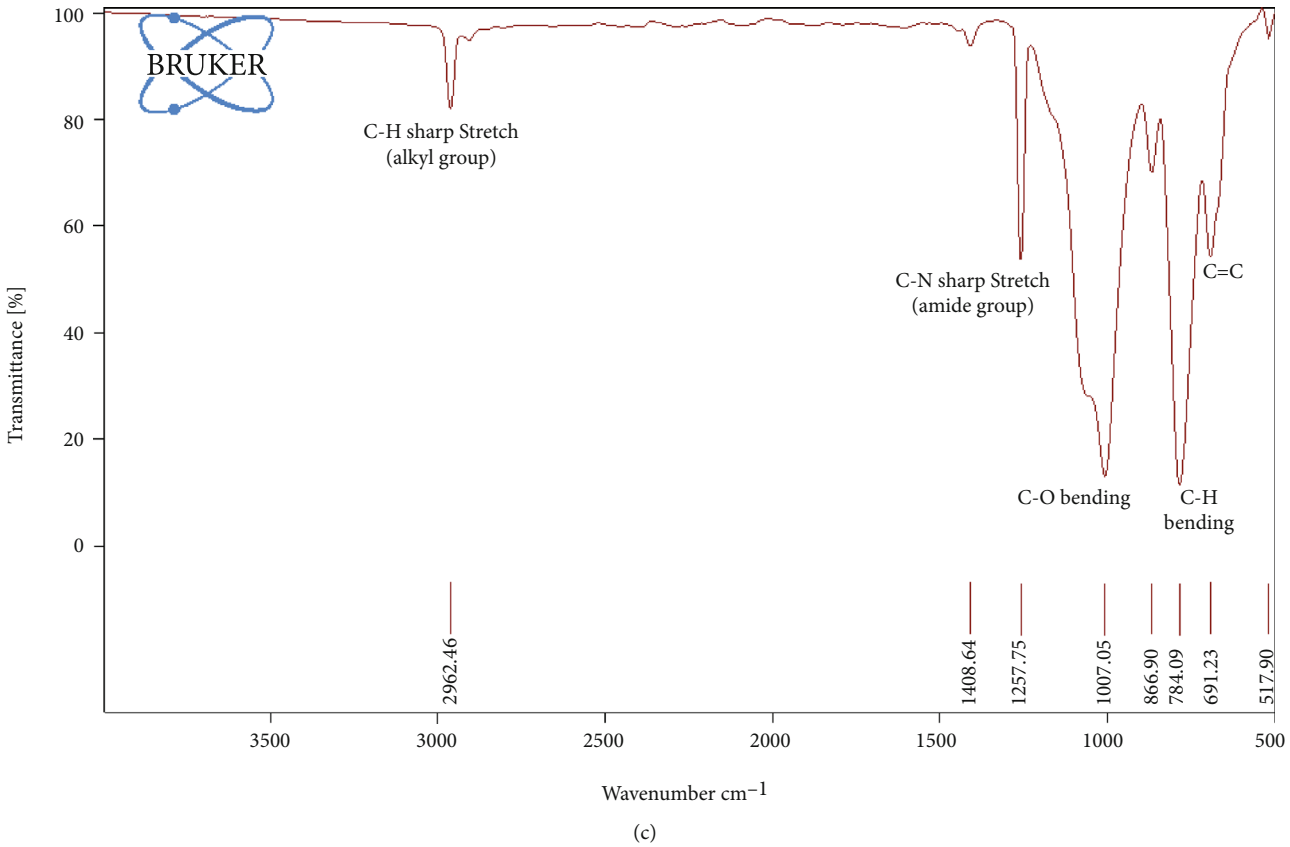

Figure 7: FTIR analysis of basalt fiber–reinforced anamide resin composites (a) 0° fiber orientation, (b) 30° fiber orientation, and (c) 45° fiber orientation.

relaxation transformation as there would be greater chain mobility, which yields less stiffness. It can be observed that on fiber loading, the storage modulus decreases, and the lowest value was identified for composite orientations of 45°.

The loss modulus defines the strain divided by the strain as stress out of phase. It is the energy factor intemperate as heat per cycle subjected to deformation that constitutes the material's viscous reaction. Figure 3 shows the variation in the loss modulus (E'') for different composite systems with temperature. From such statistics, it becomes obvious that the addition of polyimide resin allows the loss modulus rate to increase. It may be due to the suppression of relaxing mechanism contained by the composites as a significance of a greater volume of chain segments after inclusion of fiber. On the specific fiber direction, this is largely in account of the segmental in control of the matrix chain on the fiber sheet, and there is an obvious change in the glassy transition temperature (T_g) towards higher temperature. The strong basalt fiber modulus imposes restrictions on the polymer molecules' segmented mobility.

The ratio of loss modulus to storage modulus is referred to as mechanical loss factor or tanδ. The material's damping properties give a polymeric system a transition between elastic and viscous phases. Damping in composites is influenced by the incorporation, type distribution, and orientation of fibers, as well as the interaction between fiber and matrix. This was found as the temperature increases, the damping values in the transition area reach a limit and then decline in the rubbery zone. Deformations are primarily elastic, and the viscous flow resulting molecular slips are low. The position and height of the tanδ peak are indicative of the structure and properties of specific composite material. Composites typically provide considerably less damping relative to smooth resin in the transfer area, as the fibers bear a larger amount of load and require only a limited part of it to strain the interface. From Figure 4, it is clear that the composite's glass transformation temperature might happen at a temperature greater than 300°C, while the composite's glassy condition is shown just below 300°C.

3.2. Effect of Fiber Orientation on Thermal Stability of Composites. In order to test the thermal deterioration of basalt fiber–reinforced anamide composite in a broad range of temperatures, TGA and DSC were performed. The composite plates undergo pyrolysis process in nitrogen-protective gaseous atmosphere [21]. Residual mass, DTG peak temperature, and char yield temperature were evaluated for the decomposition process. Under specific fiber orientation, a single phase decomposition method was tested for all composites. Figure 5 shows a single stage degradation cycle with 0° fiber orientation for basalt fiber–reinforced polymer composites. The DTA peak was observed to be at a temperature of 608.9°C resulting from endothermic reaction with a residual mass of 92.98% remaining at 726.2°C

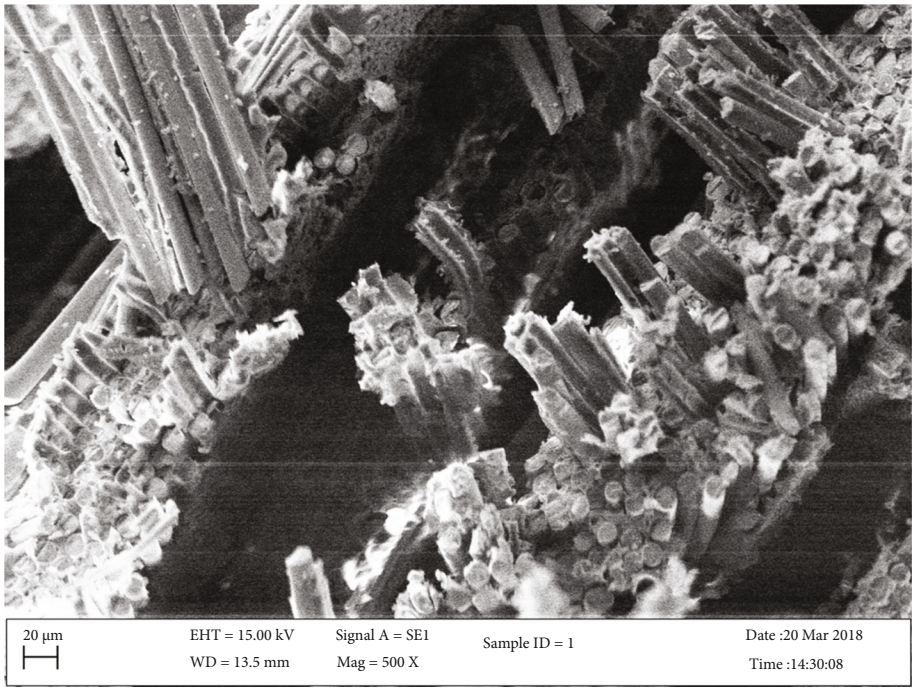

(a)

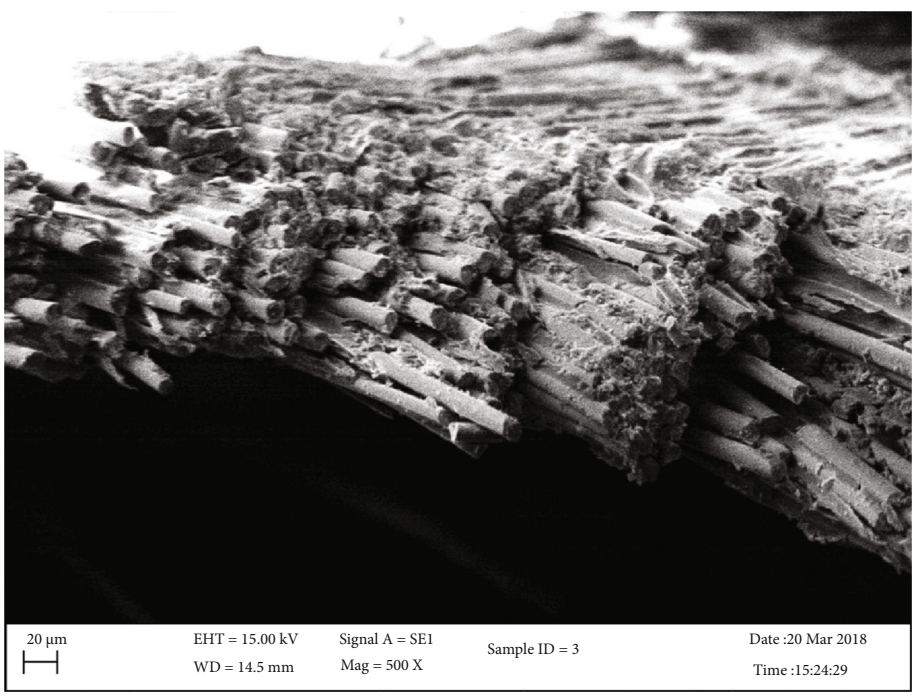

(b)

Figure 8: Continued.

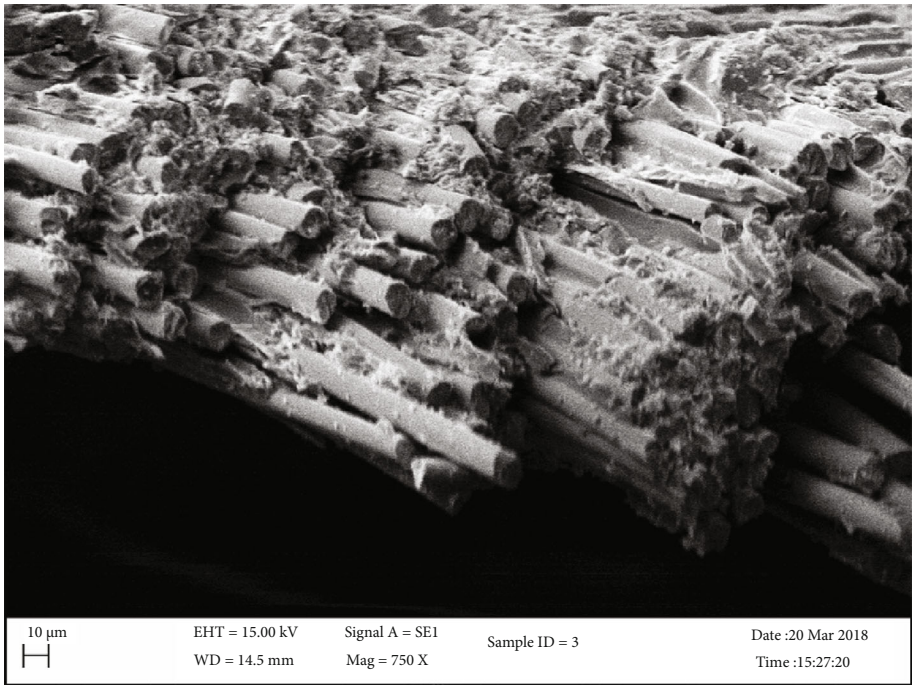

(c)

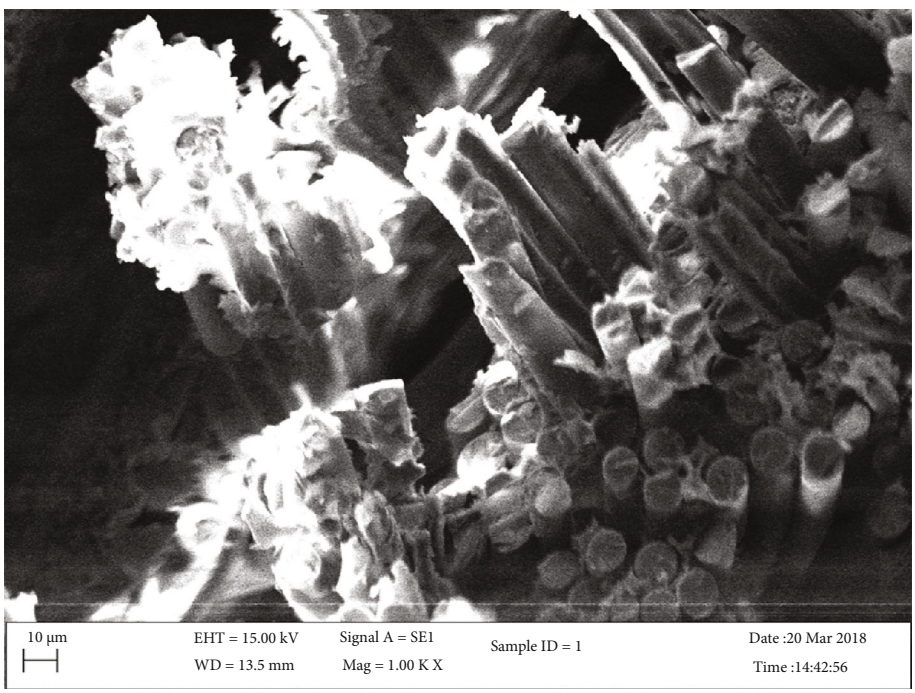

(d)

Figure 8: Scanning electron microscopic images of basalt fiber–reinforced with anamide composites. (a) Fiber pull out at 0o orientation. (b) Fiber resin bonding. (c) Fiber resin bonding at higher magnification. (d) Fiber debonding at 45o orientation.

after burning off the char yield. The temperature to extrapolate begins at 567°C level. The composites melting enthalpy under 0° fiber orientation was measured as 185 J/g. The marginal mass loss was reported before the temperature initiation after which it slowly increased to 7.02% with temperature rise and heat absorption. Thermal endurance at different orientations is mentioned in Table 3. After the melting area, the rise in heat absorption is attributed to the absorption of gaseous substances, such as charcoal or char yield with a tight C=C bond.

Figure 6, which decreases the residual mass for the fiber orientation from 0 to 30°, raises the melting peak temperature to 703.7°C owing to the reverse exothermic reaction, is assumed. The drop in mass from the sample heated to the

initial sample mass in nitrogen gas is noticed at 959.1°C to 86.70%. A steady weight reduction was initially reported until it falls at an inflection temperature of 583.6°C to 8.96%. Amid steady temperature rise at consistent heating, the mass loss rose from 8.96 to 13.70% with a temperature rise of about 400°C. The 30° fiber centered composite plate's melting enthalpy was measured at 3754 J/g, with an improvement in the heat absorption field.

A distinct characteristic of two-stage decomposition is found in the thermal study of composite anamide reinforced with 45° fiber-oriented basalt fiber, as seen in Figure 6, which shows that the first step of decomposition happens at a temperature of 94.5°C, leading to the condensation of the frame resulting in the release of volatile and the second level of decomposition at a maximum peak temperature of 630.9°C with 2998 J/g maximum enthalpy leading to polymer chain carbonisation. There was a mass loss of 4.90% at the initial decomposition step, which slowly rose as the temperature increased. For the composites second stage of decomposition, the inflection point was observed at 609.9°C. The DTA peak was found to be at 908.6°C with 83.90% of the residual mass left. A total weight loss of 16.10% occurred due to an increase in the orientation of the fiber.

3.3. FTIR Analysis of Fiber Composites. Spectroscopic analysis of FTIR was performed to confirm the presence of polar functional groups on the composites reinforced with basalt fiber. The FTIR studies of the strengthened basalt anamide composites is known from the graph seen in Figure 7(a) 0° fiber orientation (b) 30° fiber orientation, and (c) 45° fiber orientation replacing a different C–H alkyl community at a transmittance spectrum of approximately 2900 cm^{-1} over wavelength. Often connected to the C–N stretch, polar amide community was located across the 1200–1300 cm^{-1} band wavelength spectrum. In fact, the in-plane C–O stretch is observed about 1000 cm^{-1} at wave level. The functional C–H index stretch was confirmed at wave number 790 cm^{-1} from the plane of 1,3 di-substituted trimethyl group. C=C functional carbonylbis (imide carbonyl group) at wave number 690 cm^{-1} is likewise shown. In the wavelength area between 1000 and 1500 cm^{-1} [22], the primary amine groups, such as the $-NH_2$ groups, were also identified. In the polymer chain, unimidized functional groups, such as the carboxyl and amide group, have been established, which could increase the resin's molten versatility during thermal processing [23].

3.4. SEM Characterization. Figure 8 displays SEM images of anamide matrix with basalt fiber. In all orientations, the polyimide resins were densely covered with a polymer film that could be clearly seen from the SEM images with high magnification. Since the introduction of polymers, the basalt fiber retained its balanced shape. The side (length-wise) scanning electron micrograph of the fibers is far greater in diameter than most traditional natural or synthetic fibers. High-imide content makes the fiber resistant to burning, microbial attack, and absorption/swelling of moisture. The basalt fibers are explicitly seen to be parallel driven. Even the inter-laminar detachment fracture along the strengthened path of the fiber was found.

Figure 8 also describes the general morphology of the specimen's fracture base. Delaminations of all the layers revealed a fracture, which was absolutely uncoupled. The 45° ply failure function reveals that fiber debonding was disrupted a few diameters long by deep matrix cracks. As a consequence of fiber bridging, few fiber splits were found in the 45° ply. The interfacial power determines if the prevailing mode of failure was matrix hackle or system de-bonding. A comparatively strong basalt/polyimide interface intensity causes the fractures to migrate through the matrix, rather than in the fiber/matrix layer, which generates hackles in the matrix. Conversely, a weak power contributes to the de-bonding phenomenon. The fiber pull out process was clearly shown, some broken fibers were uncovered without the matrix bundle, and some matrix was left with a large fiber-shaped opening.

The mechanism has been disclosed in its entirety, some defragmented fibers have been found exposed outside of the matrix packaging, and some matrix has been found with a large hole in the shape of a fiber. In the end, it was discovered that a rise in temperature causes the complicated processes of the various directed laminates to consist of delamination, fiber breakage, matrix fracture, and fiber/matrix interface de-bonding in each direction of the plies. The gradual increase in temperature of the basalt and anamide prepeg resulted in an increase in void.

4. Conclusion

This research measured the thermo-mechanical and functional mechanical properties of anamide composites supported by basalt. The test analysis obtained showed that increased fiber orientation reduced the composite's dimensional and thermal resilience. The basalt fiber–reinforced anamide reinforcement compression modulus is higher with few fiber orientation. From the graphs, it is clear that the average difference in storage module at 1 Hz frequency is about 4250, 2900, and 2550 MPa for 0, 30, and 45° fiber orientations, respectively. This is because the increase in fiber orientation leads to a change in the contact area between anamide resin and reinforced basalt fibers, which ultimately affects the effectual transfer of stress between basalt fiber and anamide composites. Similarly, a change in glass transfer temperature to left above 300°C coincided with a rise in basalt fiber–reinforced anamide composites fiber angle.

Data Availability

All data used to support the findings of this study are included within the article.

Conflicts of Interest

The authors declare that they have no conflicts of interest.

Acknowledgments

The authors would like to thank Department of Mechanical Engineering, St. Joseph's College of Engineering, Chennai, Tamil Nadu, India, for providing facility to carry out this research work.

References

[1] M. Masuelli, *Fiber Reinforced Polymers: The Technology Applied for Concrete Repair: BoD–Books on Demand*, IntechOpen, London, 2013.

[2] D. G. Seong, C. Kang, S. Y. Pak, C. H. Kim, and Y. S. Song, "Influence of fiber length and its distribution in three phase poly(propylene) composites," *Composites Part B: Engineering*, vol. 168, no. 3, pp. 218–225, 2019.

[3] J. Lienhard and L. Schulenberg, "Strain rate dependent multiaxial characterization of long fiber reinforced plastic," *Composites Part B: Engineering*, vol. 141, pp. 164–173, 2018.

[4] S. Bartus and U. Vaidya, "Performance of long fiber reinforced thermoplastics subjected to transverse intermediate velocity blunt object impact," *Composite Structures*, vol. 67, no. 3, pp. 263–277, 2005.

[5] Y. Zhang, C. Yu, P. K. Chu et al., "Mechanical and thermal properties of basalt fiber reinforced poly(butylene succinate) composites," *Materials Chemistry and Physics*, vol. 133, no. 2–3, pp. 845–849, 2012.

[6] P. R. V. Doddi, R. Chanamala, and S. P. Dora, "Investigations on the influence of laminate angle on the damping performance of cross-ply natural composites," *Journal of Materials Engineering and Performance*, vol. 30, no. 2, pp. 1039–1045, 2021.

[7] Z. Lu, G. Xian, and H. Li, "Effects of elevated temperatures on the mechanical properties of basalt fibers and BFRP plates," *Construction and Building Materials*, vol. 127, pp. 1029–1036, 2016.

[8] D. S. Prasad, N. S. Ebenezer, C. Shoba, and S. R. Pujari, "Effect of nickel electroplating on the mechanical damping and storage modulus of metal matrix composites," *Materials Research Express*, vol. 5, no. 11, article 116409, 2018.

[9] D. S. Prasad and C. Shoba, "Damping behavior of metal matrix composites," *Transactions of the Indian Institute of Metals*, vol. 68, no. 2, pp. 161–167, 2015.

[10] D. S. Prasad, P. T. Radha, C. Shoba, and P. S. Rao, "Dynamic mechanical behavior of WC-Co coated A356.2 aluminum alloy," *Journal of Alloys and Compounds*, vol. 767, pp. 988–993, 2018.

[11] N. Saba, M. Jawaid, O. Y. Alothman, and M. T. Paridah, "A review on dynamic mechanical properties of natural fibre reinforced polymer composites," *Construction and Building Materials*, vol. 106, pp. 149–159, 2016.

[12] M. K. Gupta and V. Deep, "Effect of stacking sequence on flexural and dynamic mechanical properties of hybrid sisal/glass polyester composite," *American Journal of Polymer Science & Engineering*, vol. 5, pp. 53–62, 2017.

[13] E. H. Portella, D. Romanzini, C. C. Angrizani, S. C. Amico, and A. J. Zattera, "Influence of stacking sequence on the mechanical and dynamic mechanical properties of cotton/glass fiber reinforced polyester composites," *Materials Research*, vol. 19, no. 3, pp. 542–547, 2016.

[14] L. M. Dana, S. F. Bou, and R. B. Gimeno, "Effects of fibre orientation and content on the mechanical, dynamic mechanical and thermal expansion properties of multi-layered glass/carbon fibre-reinforced polymer composites," *Journal of Composite Materials*, vol. 49, no. 10, pp. 1211–1221, 2015.

[15] A. N. Mengal and S. Karuppanan, "Influence of angle ply orientation on the flexural strength of basalt and carbon fiber reinforced hybrid composites," *Composites Research*, vol. 28, no. 1, pp. 1–5, 2015.

[16] M. K. Gupta, "Effect of frequencies on dynamic mechanical properties of hybrid jute/sisal fibre reinforced epoxy composite," *Advances in Materials and Processing Technologies*, vol. 3, no. 4, pp. 651–664, 2017.

[17] V. I. N. C. E. N. Z. O. Fiore, G. Di Bella, and A. Valenza, "Glass-basalt/epoxy hybrid composites for marine applications," *Materials & Design*, vol. 32, no. 4, pp. 2091–2099, 2011.

[18] P. Banibayat and A. Patnaik, "Variability of mechanical properties of basalt fiber reinforced polymer bars manufactured by wet-layup method," *Materials & Design*, vol. 56, pp. 898–906, 2014.

[19] M. R. Ahmad and B. Chen, "Microstructural characterization of basalt fiber reinforced magnesium phosphate cement supplemented by silica fume," *Construction and Building Materials*, vol. 237, article 117795, 2020.

[20] P. R. Doddi, R. C. Venkata, and S. P. Dora, "Effect of fiber orientation on dynamic mechanical properties of PALF hybridized with basalt reinforced epoxy composites," *Materials Research Express*, vol. 7, no. 1, article 015329, 2020.

[21] Z. N. Azwa and B. F. Yousif, "Characteristics of kenaf fibre/epoxy composites subjected to thermal degradation," *Polymer Degradation and Stability*, vol. 98, no. 12, pp. 2752–2759, 2013.

[22] S. Yu, O. Kyung Hwan, and S. H. Hong, "Enhancement of the mechanical properties of basalt fiber-reinforced polyamide 6,6 composites by improving interfacial bonding strength through plasma-polymerization," *Composites Science and Technology*, vol. 182, article 107756, 2019.

[23] J. Xie, L. Yao, X. Fujun et al., "Fabrication and characterization of three-dimensional PMR polyimide composites reinforced with woven basalt fabric," *Composites Part B: Engineering*, vol. 66, pp. 268–275, 2014.